Stochastic Modeling of the 3D Morphologies of Energy Materials on Various Length Scales

Ole Stenzel

Ulm University

September 3, 2013

Stochastic Modeling with Applications in Materials Design

- Elucidate relationship between morphology and functionality
- Identify morphologies with improved properties

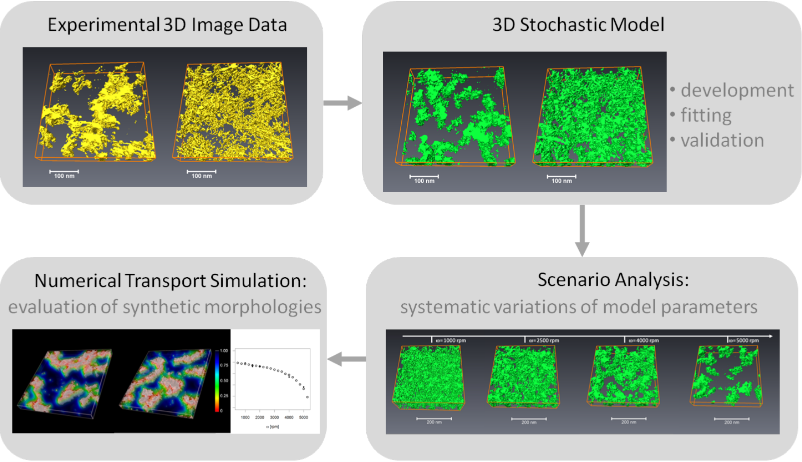

Overview

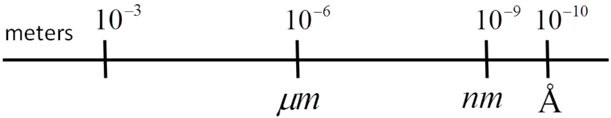

Nanoscopic length scale

- Scale: 1-100 nm
- System of molecules
- Application: organic semiconductors

Mesoscopic length scale

- Scale: 100-1000 nm
- 2-phase material (anisotropic)
- Application: organic solar cell

Microscopic length scale

- Scale: 100-1000 μm
- Application: uncompressed graphite electrode (used in Li-ion batteries)

Stochastic Modeling on Mesoscopic Length Scale and Application to Organic Solar Cells

Introduction

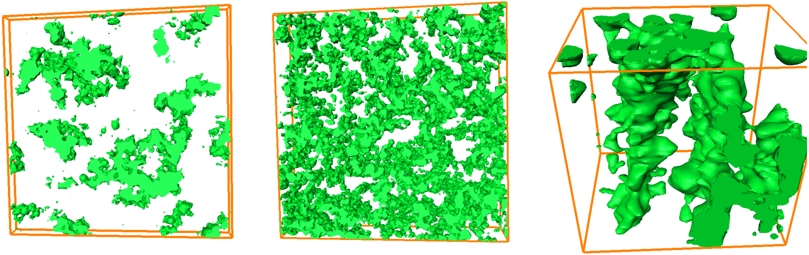

- Mesoscopic scale: 100-1000 nm

Introduction

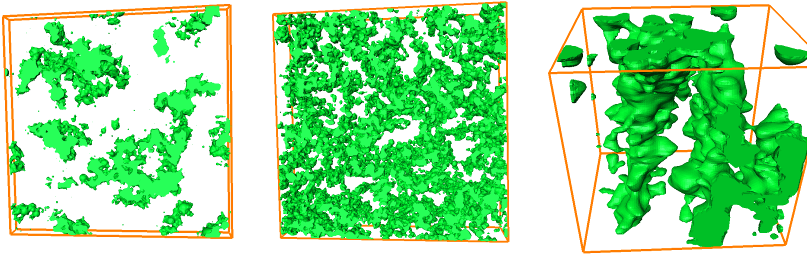

- Mesoscopic scale: 100-1000 nm
- Morphology: system of molecules, approximated by voxel grid

Introduction

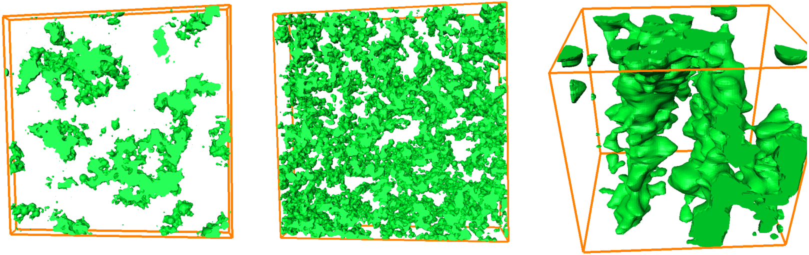

- Mesoscopic scale: 100-1000 nm
- Morphology: system of molecules, approximated by voxel grid
- goal: flexible model for complex, 2-phase anisotropic morphology
- Modeling approach: Multi-scale sphere model

Introduction

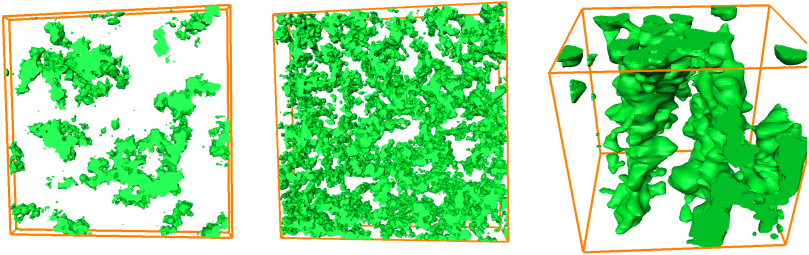

- Mesoscopic scale: 100-1000 nm
- Morphology: system of molecules, approximated by voxel grid
- goal: flexible model for complex, 2-phase anisotropic morphology
- Modeling approach: Multi-scale sphere model
- Application: elucidate relationship between morphology and efficiency (e.g. organic solar cells)

Modeling approach – Multi-scale sphere model

Modeling approach – Multi-scale sphere model

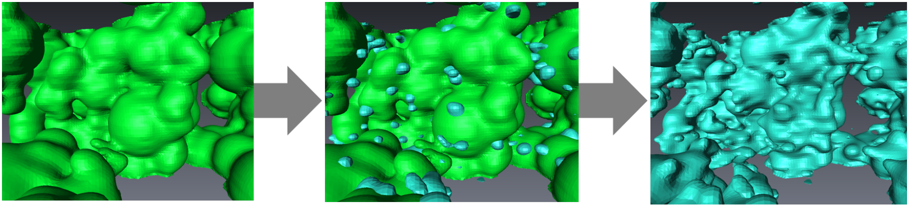

Modeling approach – Multi-scale sphere model

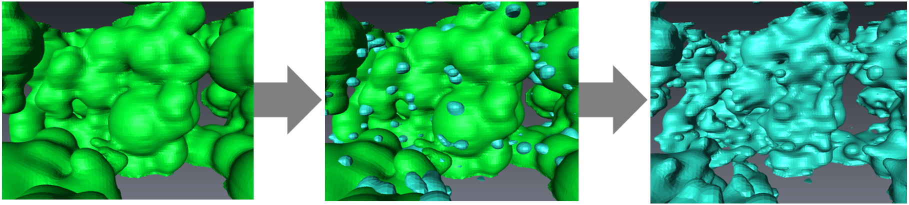

- ‘Macro’ level: sphere model (marked point process)

Modeling approach – Multi-scale sphere model

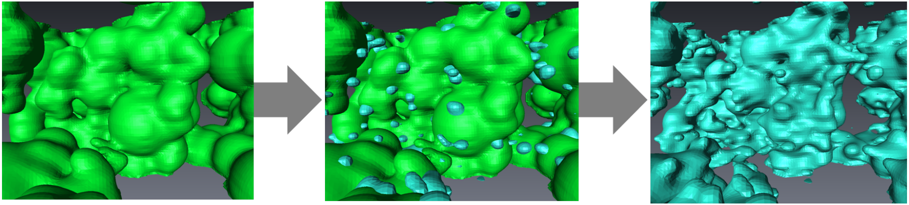

- ‘Macro’ level: sphere model (marked point process)
- ‘Micro’ level: Cox-model for spheres & erosion

‘Macro’ level: Marked point process

'Macro' level: Marked point process

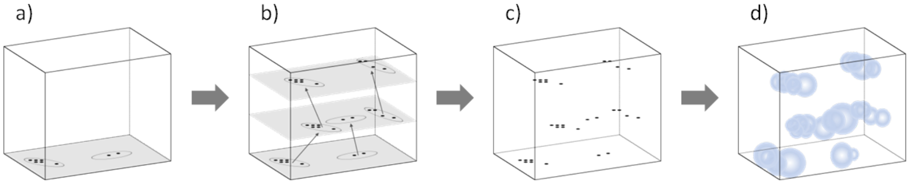

‘Macro’ level: Marked point process

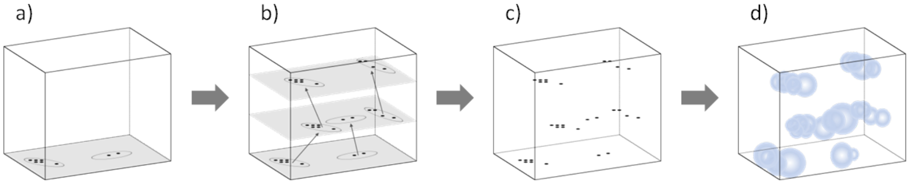

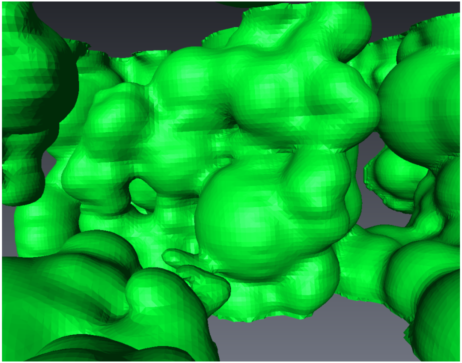

'Macro' level: Marked point process

'Macro' level: Marked point process

(i) 3D point process: Markov chain $\{\{S_n^{(z)}, n \geq 1\}, z \geq 0\}$ of 2D elliptical cluster processes

'Macro' level: Marked point process

(i) 3D point process: Markov chain $\{\{S_n^{(z)}, n \geq 1\}, z \geq 0\}$ of 2D elliptical cluster processes

- initial point process $\{S_n^{(0)}, n \geq 1\}$ in the plane $\mathbb{R} \times \mathbb{R} \times \{0\}$

'Macro' level: Marked point process

(i) 3D point process: Markov chain $\{\{S_n^{(z)}, n \geq 1\}, z \geq 0\}$ of 2D elliptical cluster processes

- initial point process $\{S_n^{(0)}, n \geq 1\}$ in the plane $\mathbb{R} \times \mathbb{R} \times \{0\}$
  - $\{T_n, n \geq 1\}$: 2D hom. Poisson process with intensity λ

'Macro' level: Marked point process

(i) 3D point process: Markov chain $\{\{S_n^{(z)}, n \geq 1\}, z \geq 0\}$ of 2D elliptical cluster processes

- initial point process $\{S_n^{(0)}, n \geq 1\}$ in the plane $\mathbb{R} \times \mathbb{R} \times \{0\}$
  - $\{T_n, n \geq 1\}$: 2D hom. Poisson process with intensity λ
  - $\mathrm{E}_{a,b}(x, \alpha)$: ellipse with axes a, b, center x, angle α

'Macro' level: Marked point process

(i) 3D point process: Markov chain $\{\{S_n^{(z)}, n \geq 1\}, z \geq 0\}$ of 2D elliptical cluster processes

- initial point process $\{S_n^{(0)}, n \geq 1\}$ in the plane $\mathbb{R} \times \mathbb{R} \times \{0\}$
  - $\{T_n, n \geq 1\}$: 2D hom. Poisson process with intensity λ
  - $\mathrm{E}_{a,b}(x, \alpha)$: ellipse with axes a, b, center x, angle α
  - $\{\psi_n, n \geq 1\}$: iid $\sim \mathrm{U}[0, \pi)$

'Macro' level: Marked point process

(i) 3D point process: Markov chain $\{\{S_n^{(z)}, n \geq 1\}, z \geq 0\}$ of 2D elliptical cluster processes

- initial point process $\{S_n^{(0)}, n \geq 1\}$ in the plane $\mathbb{R} \times \mathbb{R} \times \{0\}$
  - $\{T_n, n \geq 1\}$: 2D hom. Poisson process with intensity λ
  - $\mathrm{E}_{a,b}(x, \alpha)$: ellipse with axes a, b, center x, angle α
  - $\{\psi_n, n \geq 1\}$: iid $\sim \mathrm{U}[0, \pi)$
  - $\{S_{ni}, i \geq 1\}, n \geq 1$: 2D hom. Poisson process with intensity λ_c

'Macro' level: Marked point process

(i) 3D point process: Markov chain $\{\{S_n^{(z)}, n \geq 1\}, z \geq 0\}$ of 2D elliptical cluster processes

- initial point process $\{S_n^{(0)}, n \geq 1\}$ in the plane $\mathbb{R} \times \mathbb{R} \times \{0\}$
  - $\{T_n, n \geq 1\}$: 2D hom. Poisson process with intensity λ
  - $\mathrm{E}_{a,b}(x, \alpha)$: ellipse with axes a, b, center x, angle α
  - $\{\psi_n, n \geq 1\}$: iid $\sim \mathrm{U}[0, \pi)$
  - $\{S_{ni}, i \geq 1\}, n \geq 1$: 2D hom. Poisson process with intensity λ_c
  - $\{S_n^{(0)}, n \geq 1\} = \bigcup_{n=1}^{\infty} \left(\{S_{ni},\ i \geq 1\} \cap \mathrm{E}_{a,b}(T_n, \psi_n)\right)$: Matérn Cluster process

'Macro' level: Marked point process

(i) 3D point process: Markov chain $\{\{S_n^{(z)}, n \geq 1\}, z \geq 0\}$ of 2D elliptical cluster processes

- initial point process $\{S_n^{(0)}, n \geq 1\}$ in the plane $\mathbb{R} \times \mathbb{R} \times \{0\}$
  - $\{T_n, n \geq 1\}$: 2D hom. Poisson process with intensity λ
  - $\mathrm{E}_{a,b}(x, \alpha)$: ellipse with axes a, b, center x, angle α
  - $\{\psi_n, n \geq 1\}$: iid $\sim \mathrm{U}[0, \pi)$
  - $\{S_{ni}, i \geq 1\}, n \geq 1$: 2D hom. Poisson process with intensity λ_c
  - $\{S_n^{(0)}, n \geq 1\} = \bigcup_{n=1}^{\infty} \big(\{S_{ni},\ i \geq 1\} \cap \mathrm{E}_{a,b}(T_n, \psi_n)\big)$: Matérn Cluster process
- Transition: Spatial birth- and death process

'Macro' level: Marked point process

(i) 3D point process: Markov chain $\{\{S_n^{(z)}, n \geq 1\}, z \geq 0\}$ of 2D elliptical cluster processes

- initial point process $\{S_n^{(0)}, n \geq 1\}$ in the plane $\mathbb{R} \times \mathbb{R} \times \{0\}$
  - $\{T_n, n \geq 1\}$: 2D hom. Poisson process with intensity λ
  - $\mathrm{E}_{a,b}(x, \alpha)$: ellipse with axes a, b, center x, angle α
  - $\{\psi_n, n \geq 1\}$: iid $\sim \mathrm{U}[0, \pi)$
  - $\{S_{ni}, i \geq 1\}, n \geq 1$: 2D hom. Poisson process with intensity λ_c
  - $\{S_n^{(0)}, n \geq 1\} = \bigcup_{n=1}^{\infty} \left(\{S_{ni},\ i \geq 1\} \cap \mathrm{E}_{a,b}(T_n, \psi_n)\right)$: Matérn Cluster process
- Transition: Spatial birth- and death process
  - $\{\delta_n^{(z)}, n \geq 1\}, z \geq 1$: death of clusters ($P(\delta_n^{(z)} = 1) = p$)

‘Macro’ level: Marked point process

(i) 3D point process: Markov chain $\{\{S_n^{(z)}, n \geq 1\}, z \geq 0\}$ of 2D elliptical cluster processes

- initial point process $\{S_n^{(0)}, n \geq 1\}$ in the plane $\mathbb{R} \times \mathbb{R} \times \{0\}$
  - $\{T_n, n \geq 1\}$: 2D hom. Poisson process with intensity λ
  - $\mathrm{E}_{a,b}(x, \alpha)$: ellipse with axes a, b, center x, angle α
  - $\{\psi_n, n \geq 1\}$: iid $\sim \mathrm{U}[0, \pi)$
  - $\{S_{ni}, i \geq 1\}, n \geq 1$: 2D hom. Poisson process with intensity λ_c
  - $\{S_n^{(0)}, n \geq 1\} = \bigcup_{n=1}^{\infty} \left(\{S_{ni},\ i \geq 1\} \cap \mathrm{E}_{a,b}(T_n, \psi_n)\right)$: Matérn Cluster process
- Transition: Spatial birth- and death process
  - $\{\delta_n^{(z)}, n \geq 1\}, z \geq 1$: death of clusters ($P(\delta_n^{(z)} = 1) = p$)
  - $\{D_n^{(z)}, n \geq 1\}, z \geq 1$: iid transition vectors

'Macro' level: Marked point process

(i) 3D point process: Markov chain $\{\{S_n^{(z)}, n \geq 1\}, z \geq 0\}$ of 2D elliptical cluster processes

- initial point process $\{S_n^{(0)}, n \geq 1\}$ in the plane $\mathbb{R} \times \mathbb{R} \times \{0\}$
  - $\{T_n, n \geq 1\}$: 2D hom. Poisson process with intensity λ
  - $\mathrm{E}_{a,b}(x, \alpha)$: ellipse with axes a, b, center x, angle α
  - $\{\psi_n, n \geq 1\}$: iid $\sim \mathrm{U}[0, \pi)$
  - $\{S_{ni}, i \geq 1\}, n \geq 1$: 2D hom. Poisson process with intensity λ_c
  - $\{S_n^{(0)}, n \geq 1\} = \bigcup_{n=1}^{\infty} (\{S_{ni},\ i \geq 1\} \cap \mathrm{E}_{a,b}(T_n, \psi_n))$: Matérn Cluster process
- Transition: Spatial birth- and death process
  - $\{\delta_n^{(z)}, n \geq 1\}, z \geq 1$: death of clusters ($P(\delta_n^{(z)} = 1) = p$)
  - $\{D_n^{(z)}, n \geq 1\}, z \geq 1$: iid transition vectors
  - $\{B_n^{(z)}, n \geq 1\}, z \geq 1$: 2D hom. Poisson process with intensity λ' ($\lambda p + \lambda' = \lambda$)

‘Macro’ level: Marked point process

(i) 3D point process: Markov chain $\{\{S_n^{(z)}, n \geq 1\}, z \geq 0\}$ of 2D elliptical cluster processes

- initial point process $\{S_n^{(0)}, n \geq 1\}$ in the plane $\mathbb{R} \times \mathbb{R} \times \{0\}$
  - $\{T_n, n \geq 1\}$: 2D hom. Poisson process with intensity λ
  - $\mathrm{E}_{a,b}(x, \alpha)$: ellipse with axes a, b, center x, angle α
  - $\{\psi_n, n \geq 1\}$: iid $\sim \mathrm{U}[0, \pi)$
  - $\{S_{ni}, i \geq 1\}, n \geq 1$: 2D hom. Poisson process with intensity λ_c
  - $\{S_n^{(0)}, n \geq 1\} = \bigcup_{n=1}^{\infty} \left(\{S_{ni},\ i \geq 1\} \cap \mathrm{E}_{a,b}(T_n, \psi_n)\right)$: Matérn Cluster process
- Transition: Spatial birth- and death process
  - $\{\delta_n^{(z)}, n \geq 1\}, z \geq 1$: death of clusters ($P(\delta_n^{(z)} = 1) = p$)
  - $\{D_n^{(z)}, n \geq 1\}, z \geq 1$: iid transition vectors
  - $\{B_n^{(z)}, n \geq 1\}, z \geq 1$: 2D hom. Poisson process with intensity λ' ($\lambda p + \lambda' = \lambda$)
  - $\{S_{ni}^{(z)}, i \geq 1\}, n, z \geq 1$: 2D hom. Poisson process with intensity λ_c

'Macro' level: Marked point process

(i) 3D point process: Markov chain $\{\{S_n^{(z)}, n \geq 1\}, z \geq 0\}$ of 2D elliptical cluster processes

- initial point process $\{S_n^{(0)}, n \geq 1\}$ in the plane $\mathbb{R} \times \mathbb{R} \times \{0\}$
  - $\{T_n, n \geq 1\}$: 2D hom. Poisson process with intensity λ
  - $\mathrm{E}_{a,b}(x, \alpha)$: ellipse with axes a, b, center x, angle α
  - $\{\psi_n, n \geq 1\}$: iid $\sim \mathrm{U}[0, \pi)$
  - $\{S_{ni}, i \geq 1\}, n \geq 1$: 2D hom. Poisson process with intensity λ_c
  - $\{S_n^{(0)}, n \geq 1\} = \bigcup_{n=1}^{\infty} \left(\{S_{ni},\ i \geq 1\} \cap \mathrm{E}_{a,b}(T_n, \psi_n)\right)$: Matérn Cluster process
- Transition: Spatial birth- and death process
  - $\{\delta_n^{(z)}, n \geq 1\}, z \geq 1$: death of clusters $(P(\delta_n^{(z)} = 1) = p)$
  - $\{D_n^{(z)}, n \geq 1\}, z \geq 1$: iid transition vectors
  - $\{B_n^{(z)}, n \geq 1\}, z \geq 1$: 2D hom. Poisson process with intensity λ' $(\lambda p + \lambda' = \lambda)$
  - $\{S_{ni}^{(z)}, i \geq 1\}, n, z \geq 1$: 2D hom. Poisson process with intensity λ_c
  - $\{S_n^{(2)}, n \geq 1\} = \bigcup_{j:\delta_j^{(1)}=1} \left(\{S_{ji} + D_j^{(1)},\ i \geq 1\} \cap \mathrm{E}_{a,b}(T_j + D_j^{(1)}, \psi_j)\right)$

$$\cup \bigcup_{n=1}^{\infty} \left(\{S_{ni}^{(1)},\ i \geq 1\} \cap \mathrm{E}_{a,b}(B_n^{(1)}, \psi_n^{(1)})\right)$$

'Macro' level: Marked point process

(i) 3D point process: Markov chain $\{\{S_n^{(z)}, n \geq 1\}, z \geq 0\}$ of 2D elliptical cluster processes

- initial point process $\{S_n^{(0)}, n \geq 1\}$ in the plane $\mathbb{R} \times \mathbb{R} \times \{0\}$
  - $\{T_n, n \geq 1\}$: 2D hom. Poisson process with intensity λ
  - $\mathrm{E}_{a,b}(x, \alpha)$: ellipse with axes a, b, center x, angle α
  - $\{\psi_n, n \geq 1\}$: iid $\sim \mathrm{U}[0, \pi)$
  - $\{S_{ni}, i \geq 1\}, n \geq 1$: 2D hom. Poisson process with intensity λ_c
  - $\{S_n^{(0)}, n \geq 1\} = \bigcup_{n=1}^{\infty} \left(\{S_{ni},\ i \geq 1\} \cap \mathrm{E}_{a,b}(T_n, \psi_n)\right)$: Matérn Cluster process
- Transition: Spatial birth- and death process
  - $\{\delta_n^{(z)}, n \geq 1\}, z \geq 1$: death of clusters $(P(\delta_n^{(z)} = 1) = p)$
  - $\{D_n^{(z)}, n \geq 1\}, z \geq 1$: iid transition vectors
  - $\{B_n^{(z)}, n \geq 1\}, z \geq 1$: 2D hom. Poisson process with intensity λ' $(\lambda p + \lambda' = \lambda)$
  - $\{S_{ni}^{(z)}, i \geq 1\}, n, z \geq 1$: 2D hom. Poisson process with intensity λ_c
  - $\{S_n^{(2)}, n \geq 1\} = \bigcup_{j:\delta_j^{(1)}=1} \left(\{S_{ji} + D_j^{(1)},\ i \geq 1\} \cap \mathrm{E}_{a,b}(T_j + D_j^{(1)}, \psi_j)\right)$
  $$\cup \bigcup_{n=1}^{\infty} \left(\{S_{ni}^{(1)},\ i \geq 1\} \cap \mathrm{E}_{a,b}(B_n^{(1)}, \psi_n^{(1)})\right)$$

b) Modeling of radii:
$R_i \sim \Gamma(\iota_{\text{shape}}, \iota_{\text{scale}})$ positively, correlated in space

‘Micro’ level: 3-stage model

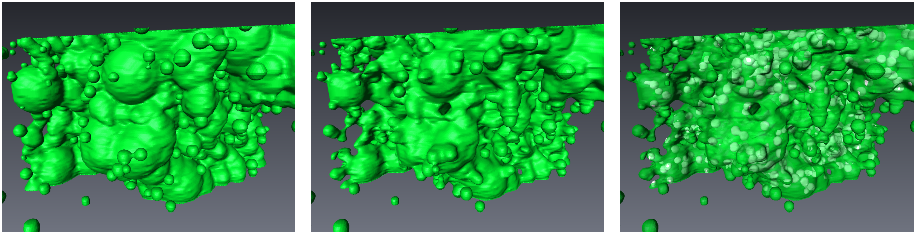

$\xi = \bigcup_{n\geq 1, z\geq 0} B(s_n^{(z)}, r_n^{(z)})$: realization of ‘macro’ model

(1) Cox sphere model: $\xi' = \xi \cup \left(\bigcup_{n\geq 1, z\geq 0} B(s_{n,\text{micro}}^{(z)}, r_{n,\text{micro}}^{(z)}) \right)$

‘Micro’ level: 3-stage model

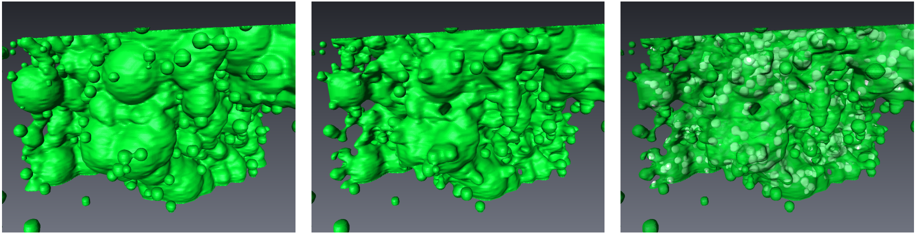

$\xi = \bigcup_{n\geq 1, z\geq 0} B(s_n^{(z)}, r_n^{(z)})$: realization of ‘macro’ model

(1) Cox sphere model: $\xi' = \xi \cup \left(\bigcup_{n\geq 1, z\geq 0} B(s_{n,\text{micro}}^{(z)}, r_{n,\text{micro}}^{(z)})\right)$

- $\{S_{n,\text{micro}}^{(z)}, n \geq 0, z \geq 1\}$ inhom. Poisson process with intensity $\lambda(x) = f(\delta_\xi(x))$.
- $\{R_{n,\text{micro}}^{(z)}, n \geq 0, z \geq 1\}$

'Micro' level: 3-stage model

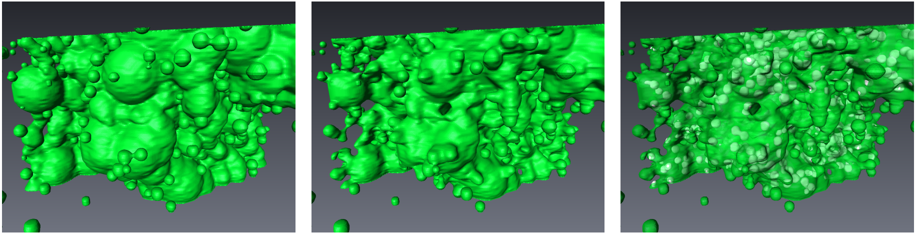

$\xi = \bigcup_{n\geq 1, z\geq 0} B(s_n^{(z)}, r_n^{(z)})$: realization of 'macro' model

(1) Cox sphere model: $\xi' = \xi \cup \left(\bigcup_{n\geq 1, z\geq 0} B(s_{n,\text{micro}}^{(z)}, r_{n,\text{micro}}^{(z)})\right)$

- $\{S_{n,\text{micro}}^{(z)}, n \geq 0, z \geq 1\}$ inhom. Poisson process with intensity $\lambda(x) = f(\delta_\xi(x))$.
- $\{R_{n,\text{micro}}^{(z)}, n \geq 0, z \geq 1\}$

(2) Erosion given $\xi' \Rightarrow \xi''$

(3) Hardcore sphere model in the inside of ξ''

Application

Application

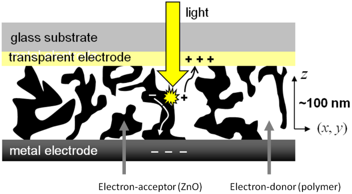

Application

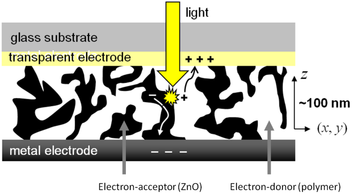

Application

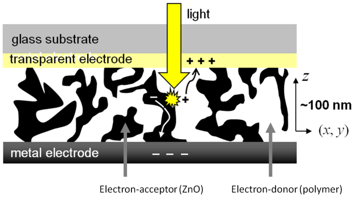

- Modeling of mesoscopic morphology of organic solar cells

Application

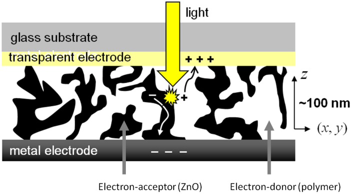

- Modeling of mesoscopic morphology of organic solar cells
- Understanding efficiency vs. morphology

Application

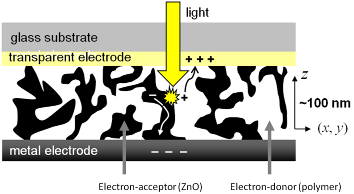

- Modeling of mesoscopic morphology of organic solar cells
- Understanding efficiency vs. morphology
- Functionality
  - device architecture: bulk heterojunction

Application

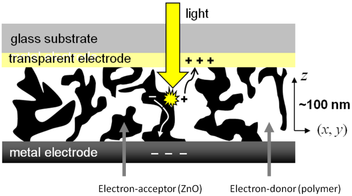

- Modeling of mesoscopic morphology of organic solar cells
- Understanding efficiency vs. morphology
- Functionality
  - device architecture: bulk heterojunction
  - light activates polymer phase

Application

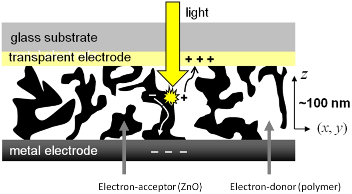

- Modeling of mesoscopic morphology of organic solar cells
- Understanding efficiency vs. morphology
- Functionality
  - device architecture: bulk heterojunction
  - light activates polymer phase
  - excitons evolve

Application

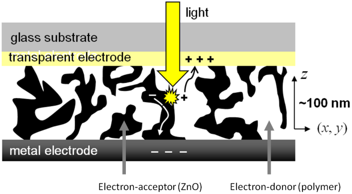

- Modeling of mesoscopic morphology of organic solar cells
- Understanding efficiency vs. morphology
- Functionality
  - device architecture: bulk heterojunction
  - light activates polymer phase
  - excitons evolve
  - diffusion of excitons in polymer phase

Application

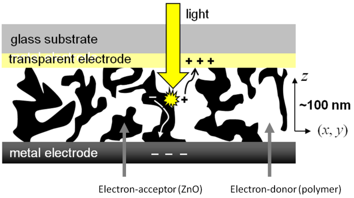

- Modeling of mesoscopic morphology of organic solar cells
- Understanding efficiency vs. morphology
- Functionality
  - device architecture: bulk heterojunction
  - light activates polymer phase
  - excitons evolve
  - diffusion of excitons in polymer phase
  - interface polymer/ZnO: quenching: exciton $\rightarrow$ electron, hole

Application

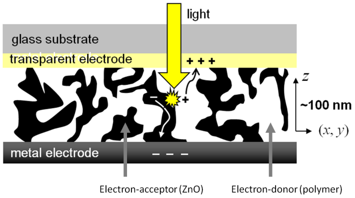

- Modeling of mesoscopic morphology of organic solar cells
- Understanding efficiency vs. morphology
- Functionality
  - device architecture: bulk heterojunction
  - light activates polymer phase
  - excitons evolve
  - diffusion of excitons in polymer phase
  - interface polymer/ZnO: quenching: exciton → electron, hole
  - charge transport towards electrodes
- Fitting to experimental 3D image data of P3HT-ZnO solar cells (TU Eindhoven)

3D image data of organic solar cells

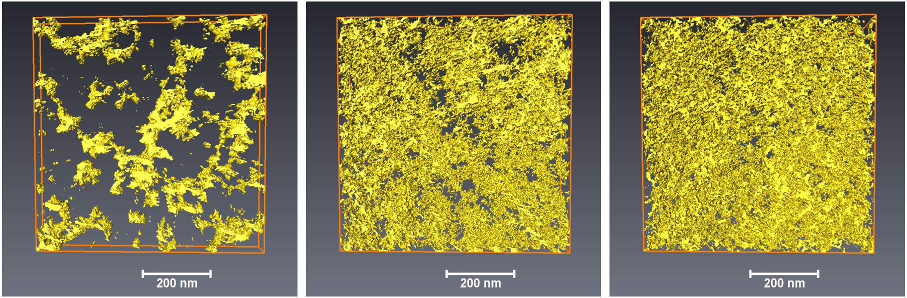

5000 rpm ∼ 57 nm   1500 rpm ∼ 100 nm   1000 rpm ∼ 167 nm

S.D. Oosterhout *et al.*, Nature Materials **8** (2009), 818–824.

- 3D TEM images of P3HT-ZnO solar cells with varying layer thicknesses
- TEM: Technical University Eindhoven
- P3HT Phase: transparent
- ZnO Phase: yellow, volume fraction 13.3% – 21.1%
- Morphology is anisotropic

Validation

Structural characteristics

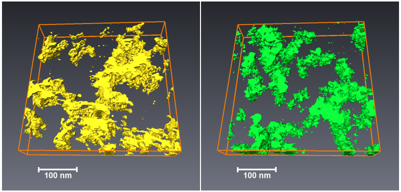

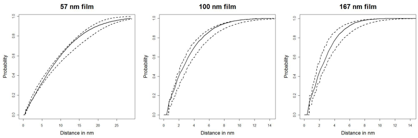

Validation

Structural characteristics

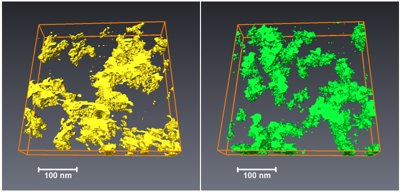

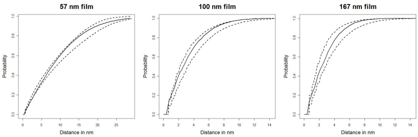

Physical characteristic

- Quenching efficiency
- $0 = \frac{dn(x)}{dt} = -\frac{n(x)}{\tau} + D\nabla^2 n(x) + g$
- D: diffusion constant, τ: exciton life time, g: rate of exciton generation
- boundary condition: $n(x) = 0$ at P3HT/ZnO interface

Validation

Structural characteristics

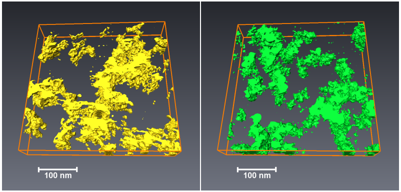

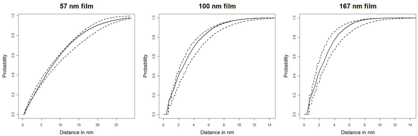

Physical characteristic

- Quenching efficiency
- $0 = \frac{dn(x)}{dt} = -\frac{n(x)}{\tau} + D\nabla^2 n(x) + g$
- D: diffusion constant, τ: exciton life time, g: rate of exciton generation
- boundary condition: $n(x) = 0$ at P3HT/ZnO interface

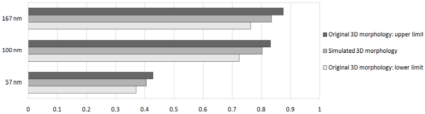

Example of application: virtual materials design

- Experimental: spin coating velocity $\omega \in [1000, 5000]$ determines morphology

Example of application: virtual materials design

- Experimental: spin coating velocity $\omega \in [1000, 5000]$ determines morphology
- Model: value model parameter λ determines morphology

Example of application: virtual materials design

- Experimental: spin coating velocity $\omega \in [1000, 5000]$ determines morphology
- Model: value model parameter λ determines morphology
- Connect ω and $\vec{\lambda}$ by non-linear regression $\lambda_i(\omega) = a_i + b_i \exp(c_i \omega) + \varepsilon_i$ or $\lambda_i(\omega) = a_i + b_i \omega + \varepsilon_i$

Example of application: virtual materials design

- Experimental: spin coating velocity $\omega \in [1000, 5000]$ determines morphology
- Model: value model parameter λ determines morphology
- Connect ω and $\vec{\lambda}$ by non-linear regression $\lambda_i(\omega) = a_i + b_i \exp(c_i \omega) + \varepsilon_i$ or $\lambda_i(\omega) = a_i + b_i \omega + \varepsilon_i$
- Analytical formula for $\vec{\lambda}$ in dependence of ω.

Example of application: virtual materials design

- Experimental: spin coating velocity $\omega \in [1000, 5000]$ determines morphology
- Model: value model parameter λ determines morphology
- Connect ω and $\vec{\lambda}$ by non-linear regression $\lambda_i(\omega) = a_i + b_i \exp(c_i\omega) + \varepsilon_i$ or $\lambda_i(\omega) = a_i + b_i\omega + \varepsilon_i$
- Analytical formula for $\vec{\lambda}$ in dependence of ω.
- Prediction of morphologies for arbitrary ω

Example of application: virtual materials design

- Experimental: spin coating velocity $\omega \in [1000, 5000]$ determines morphology
- Model: value model parameter λ determines morphology
- Connect ω and $\vec{\lambda}$ by non-linear regression $\lambda_i(\omega) = a_i + b_i \exp(c_i \omega) + \varepsilon_i$ or $\lambda_i(\omega) = a_i + b_i \omega + \varepsilon_i$
- Analytical formula for $\vec{\lambda}$ in dependence of ω.
- Prediction of morphologies for arbitrary ω

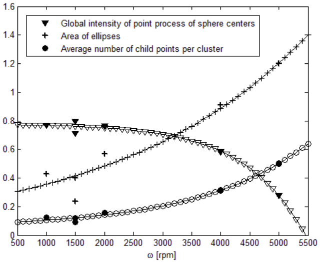

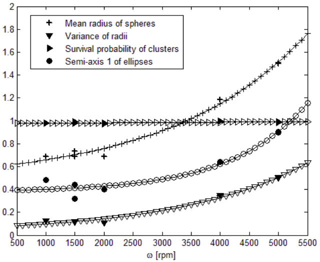

Scenario analysis

- Simulation virtual morphologies for $\omega = 500, 750, \ldots, 5250$

Scenario analysis

- Simulation virtual morphologies for $\omega = 500, 750, \ldots, 5250$
- Analysis (structure, quenching)

Scenario analysis

- Simulation virtual morphologies for $\omega = 500, 750, \ldots, 5250$
- Analysis (structure, quenching)

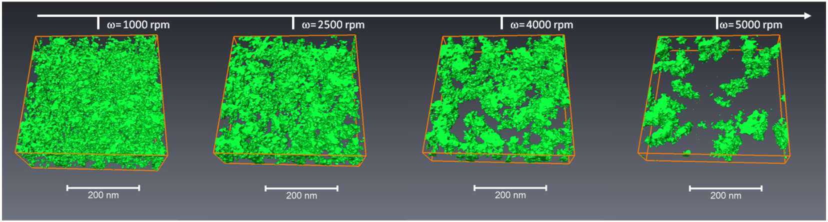

Scenario analysis

- Simulation virtual morphologies for $\omega = 500, 750, \ldots, 5250$
- Analysis (structure, quenching)

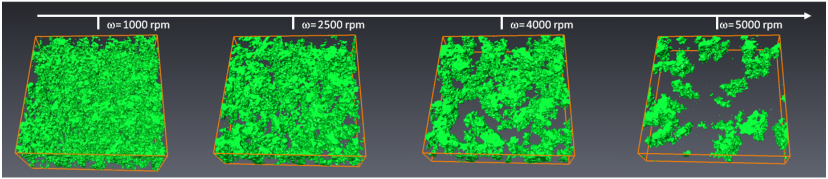

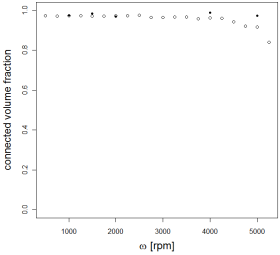

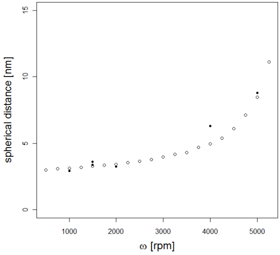

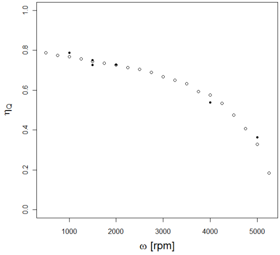

Stochastic Modeling on Nanoscopic Length Scale
and
Application to Organic Semiconductors

Introduction

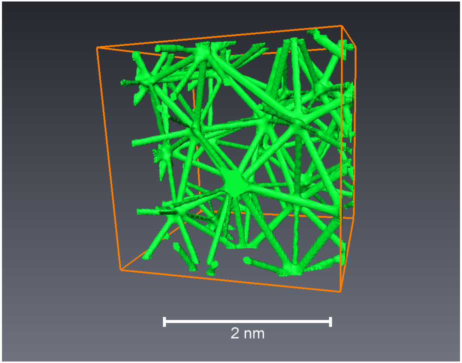

- Nanoscopic scale: 1-100 nm

Introduction

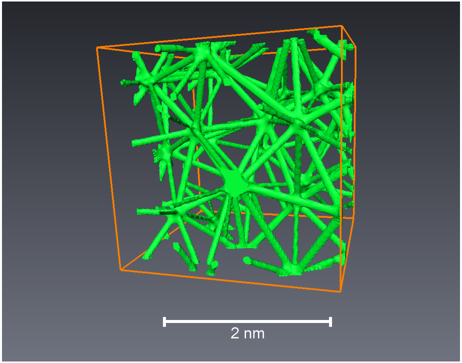

- Nanoscopic scale: 1-100 nm
- Morphology: system of molecules

Introduction

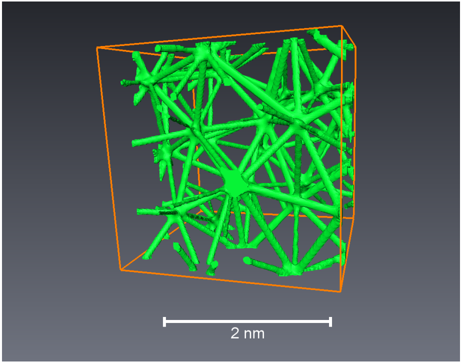

- Nanoscopic scale: 1-100 nm
- Morphology: system of molecules
- Modeling approach: random geometric graph $G = (V, E, Q)$

Introduction

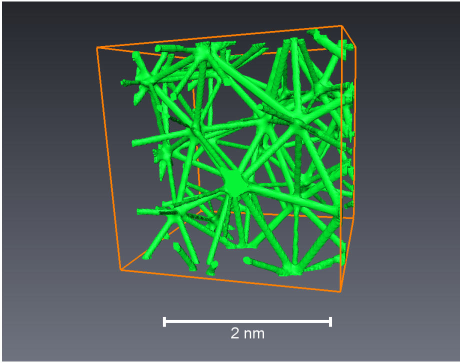

- Nanoscopic scale: 1-100 nm
- Morphology: system of molecules
- Modeling approach: random geometric graph $G = (V, E, Q)$
- Application: charge transport of holes and electrons

Introduction

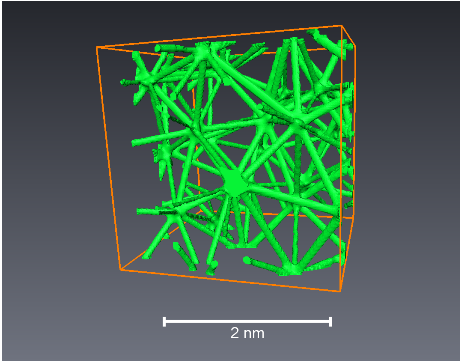

- Nanoscopic scale: 1-100 nm
- Morphology: system of molecules
- Modeling approach: random geometric graph $G = (V, E, Q)$
- Application: charge transport of holes and electrons
- Random movement of charges follows a Markov process

Modeling Approach

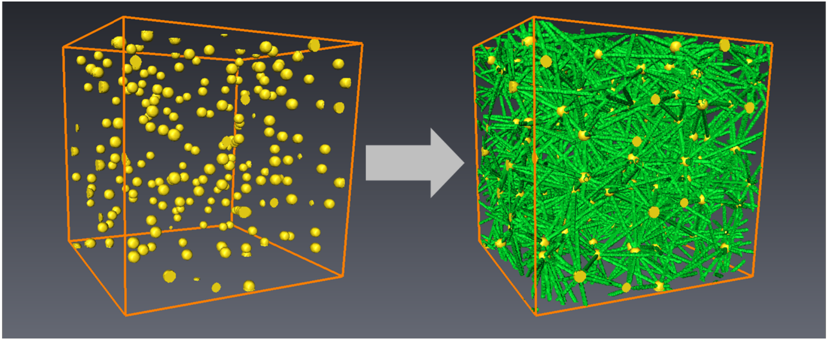

Modeling of Vertices V

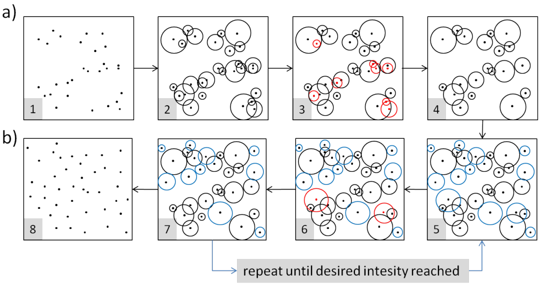

a) Dominance-Competition point process (Stoyan 1988)

Modeling of Vertices V

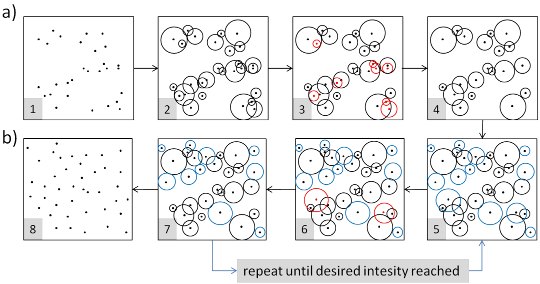

a) Dominance-Competition point process (Stoyan 1988)

- $\{S_n, n \geq 1\}$ homogeneous Poisson process, $\{L_n, n \geq 1\}$ iid, independent of $\{S_n\}$ with $L_1 : \Omega \to (0, \infty)$.

Modeling of Vertices V

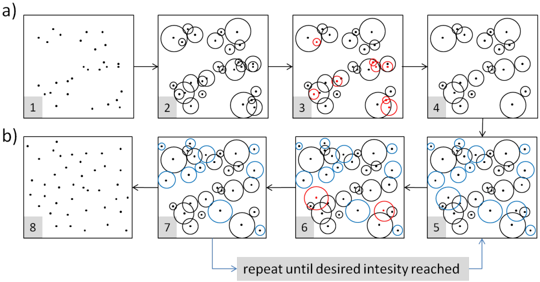

a) Dominance-Competition point process (Stoyan 1988)

- $\{S_n, n \geq 1\}$ homogeneous Poisson process, $\{L_n, n \geq 1\}$ iid, independent of $\{S_n\}$ with $L_1 : \Omega \to (0, \infty)$.
- $M_n = \begin{cases} \sup\{L_k, k \neq n : |S_k - S_n| < L_k\} & \text{if } \#\{k \neq n : |S_k - S_n| < L_k\} > 0 \\ 0 & \text{else} \end{cases}$

Modeling of Vertices V

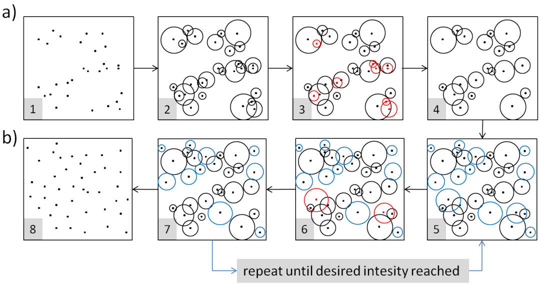

a) Dominance-Competition point process (Stoyan 1988)

- $\{S_n, n \geq 1\}$ homogeneous Poisson process, $\{L_n, n \geq 1\}$ iid, independent of $\{S_n\}$ with $L_1 : \Omega \to (0, \infty)$.
- $M_n = \begin{cases} \sup\{L_k, k \neq n : |S_k - S_n| < L_k\} & \text{if } \#\{k \neq n : |S_k - S_n| < L_k\} > 0 \\ 0 & \text{else} \end{cases}$
- point process $\{\widetilde{S}_n\}$ with $\widetilde{S}_n = \begin{cases} S_n & \text{if } L_n > M_n, \\ \infty & \text{else .} \end{cases}$

Modeling of Vertices V

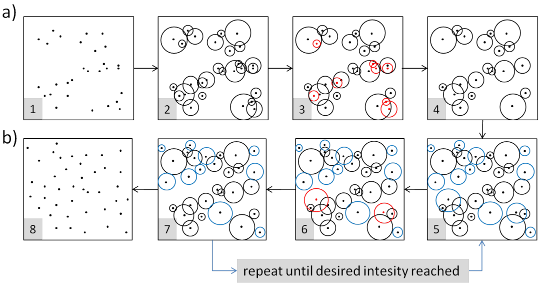

a) Dominance-Competition point process (Stoyan 1988)

- $\{S_n, n \geq 1\}$ homogeneous Poisson process, $\{L_n, n \geq 1\}$ iid, independent of $\{S_n\}$ with $L_1 : \Omega \to (0, \infty)$.
- $M_n = \begin{cases} \sup\{L_k, k \neq n : |S_k - S_n| < L_k\} & \text{if } \#\{k \neq n : |S_k - S_n| < L_k\} > 0 \\ 0 & \text{else} \end{cases}$
- point process $\{\widetilde{S}_n\}$ with $\widetilde{S}_n = \begin{cases} S_n & \text{if } L_n > M_n, \\ \infty & \text{else} . \end{cases}$

b) Extension with respect to further iterations

Modeling of Edges E

Modeling of Edges E

- Idea: connect $S_i \in V$ with nearest neighbors

Modeling of Edges E

- Idea: connect $S_i \in V$ with nearest neighbors
  - put edges (S_i, S_j) with probability $f(d(S_i, S_j))$

Modeling of Edges E

- Idea: connect $S_i \in V$ with nearest neighbors
  - put edges (S_i, S_j) with probability $f(d(S_i, S_j))$
  - $f(r) = \begin{cases} 1 & r < r_{\text{min}} \\ p_g(r) & r_{\text{min}} \leq r \leq r_{\text{max}} \\ 0 & \text{else} \end{cases}$

Modeling of Edges E

- Idea: connect $S_i \in V$ with nearest neighbors
  - put edges (S_i, S_j) with probability $f(d(S_i, S_j))$
  - $f(r) = \begin{cases} 1 & r < r_{\min} \\ p_g(r) & r_{\min} \leq r \leq r_{\max} \\ 0 & \text{else} \end{cases}$
  - p_g polynomial of degree g, decreasing

Modeling of Edges E

- Idea: connect $S_i \in V$ with nearest neighbors
  - put edges (S_i, S_j) with probability $f(d(S_i, S_j))$
  - $f(r) = \begin{cases} 1 & r < r_{\min} \\ p_g(r) & r_{\min} \le r \le r_{\max} \\ 0 & \text{else} \end{cases}$
  - p_g polynomial of degree g, decreasing
- Extension to adjust graph properties possible

Modeling of edge weights Q

- Movement of charges according to Markov process

Modeling of edge weights Q

- Movement of charges according to Markov process
- $Q = \{Q_{ij}, (S_i, S_j) \text{ oder } (S_j, S_i) \in E\}$ transition rates

Modeling of edge weights Q

- Movement of charges according to Markov process
- $Q = \{Q_{ij}, (S_i, S_j) \text{ oder } (S_j, S_i) \in E\}$ transition rates
- $Q_{ij} = \frac{2\pi}{\hbar} \frac{J_{ij}^2}{\sqrt{4\pi\lambda_{ij} k_B T}} \exp\left[-\frac{(\Delta\mathcal{E}_{ij} - \lambda_{ij})^2}{4\lambda_{ij} k_B T}\right]$

Modeling of edge weights Q

- Movement of charges according to Markov process
- $Q = \{Q_{ij}, (S_i, S_j) \text{ oder } (S_j, S_i) \in E\}$ transition rates
- $Q_{ij} = \frac{2\pi}{\hbar} \frac{J_{ij}^2}{\sqrt{4\pi\lambda_{ij} k_B T}} \exp\left[-\frac{(\Delta\mathcal{E}_{ij} - \lambda_{ij})^2}{4\lambda_{ij} k_B T}\right]$
  - J_{ij}: transfer integrals

Modeling of edge weights Q

- Movement of charges according to Markov process
- $Q = \{Q_{ij}, (S_i, S_j) \text{ oder } (S_j, S_i) \in E\}$ transition rates
- $Q_{ij} = \frac{2\pi}{\hbar} \frac{J_{ij}^2}{\sqrt{4\pi\lambda_{ij} k_B T}} \exp\left[-\frac{(\Delta\mathcal{E}_{ij} - \lambda_{ij})^2}{4\lambda_{ij} k_B T}\right]$
  - J_{ij}: transfer integrals
  - $\Delta\mathcal{E}_{ij} = \Delta\mathcal{E}^{el} + \Delta\mathcal{E}^{ext}$: energy difference

Modeling of edge weights Q

- Movement of charges according to Markov process
- $Q = \{Q_{ij}, (S_i, S_j) \text{ oder } (S_j, S_i) \in E\}$ transition rates
- $Q_{ij} = \frac{2\pi}{\hbar} \frac{J_{ij}^2}{\sqrt{4\pi\lambda_{ij} k_B T}} \exp\left[-\frac{(\Delta\mathcal{E}_{ij} - \lambda_{ij})^2}{4\lambda_{ij} k_B T}\right]$
  - J_{ij}: transfer integrals
  - $\Delta\mathcal{E}_{ij} = \Delta\mathcal{E}^{el} + \Delta\mathcal{E}^{ext}$: energy difference
  - $\Delta\mathcal{E}^{el} = \mathcal{E}_i - \mathcal{E}_j$: difference in electrostatic energy
  - $\Delta\mathcal{E}^{ext} = q < \mathbf{F}, S_i - S_j >$: energy difference due to electric field

Modeling of edge weights Q

- Movement of charges according to Markov process
- $Q = \{Q_{ij}, (S_i, S_j) \text{ oder } (S_j, S_i) \in E\}$ transition rates
- $Q_{ij} = \frac{2\pi}{\hbar} \frac{J_{ij}^2}{\sqrt{4\pi\lambda_{ij} k_B T}} \exp\left[-\frac{(\Delta\mathcal{E}_{ij} - \lambda_{ij})^2}{4\lambda_{ij} k_B T}\right]$
  - J_{ij}: transfer integrals
  - $\Delta\mathcal{E}_{ij} = \Delta\mathcal{E}^{el} + \Delta\mathcal{E}^{ext}$: energy difference
  - $\Delta\mathcal{E}^{el} = \mathcal{E}_i - \mathcal{E}_j$: difference in electrostatic energy
  - $\Delta\mathcal{E}^{ext} = q < \mathbf{F}, S_i - S_j >$: energy difference due to electric field

- Modeling of $\{\mathcal{E}_n, n \geq 1\}$

Modeling of edge weights Q

- Movement of charges according to Markov process
- $Q = \{Q_{ij}, (S_i, S_j) \text{ oder } (S_j, S_i) \in E\}$ transition rates
- $Q_{ij} = \frac{2\pi}{\hbar} \frac{J_{ij}^2}{\sqrt{4\pi\lambda_{ij} k_B T}} \exp\left[-\frac{(\Delta\mathcal{E}_{ij} - \lambda_{ij})^2}{4\lambda_{ij} k_B T}\right]$
  - J_{ij}: transfer integrals
  - $\Delta\mathcal{E}_{ij} = \Delta\mathcal{E}^{el} + \Delta\mathcal{E}^{ext}$: energy difference
  - $\Delta\mathcal{E}^{el} = \mathcal{E}_i - \mathcal{E}_j$: difference in electrostatic energy
  - $\Delta\mathcal{E}^{ext} = q < \mathbf{F}, S_i - S_j >$: energy difference due to electric field

- Modeling of $\{\mathcal{E}_n, n \geq 1\}$
  - $\mathcal{E}_n \sim \mathcal{N}(m_{\mathcal{E}}, \sigma_{\mathcal{E}}^2)$ positively correlated in space:

Modeling of edge weights Q

- Movement of charges according to Markov process
- $Q = \{Q_{ij}, (S_i, S_j) \text{ oder } (S_j, S_i) \in E\}$ transition rates
- $Q_{ij} = \frac{2\pi}{\hbar} \frac{J_{ij}^2}{\sqrt{4\pi\lambda_{ij} k_B T}} \exp\left[-\frac{(\Delta\mathcal{E}_{ij} - \lambda_{ij})^2}{4\lambda_{ij} k_B T}\right]$
  - J_{ij}: transfer integrals
  - $\Delta\mathcal{E}_{ij} = \Delta\mathcal{E}^{\text{el}} + \Delta\mathcal{E}^{\text{ext}}$: energy difference
  - $\Delta\mathcal{E}^{\text{el}} = \mathcal{E}_i - \mathcal{E}_j$: difference in electrostatic energy
  - $\Delta\mathcal{E}^{\text{ext}} = q < \mathbf{F}, S_i - S_j >$: energy difference due to electric field

- Modeling of $\{\mathcal{E}_n, n \geq 1\}$
  - $\mathcal{E}_n \sim \mathcal{N}(m_{\mathcal{E}}, \sigma_{\mathcal{E}}^2)$ positively correlated in space:
  - $M_n^{(a)}, M_n^{(b)}, M_n^{(c)} \sim \mathcal{N}(0, \sigma_{\mathcal{E}}^2)$ iid $\Rightarrow$ 4−tuple $(S_n, M_n^{(a)}, M_n^{(b)}, M_n^{(c)})$

Modeling of edge weights Q

- Movement of charges according to Markov process
- $Q = \{Q_{ij}, (S_i, S_j) \text{ oder } (S_j, S_i) \in E\}$ transition rates
- $Q_{ij} = \frac{2\pi}{\hbar} \frac{J_{ij}^2}{\sqrt{4\pi\lambda_{ij} k_B T}} \exp\left[-\frac{(\Delta\mathcal{E}_{ij} - \lambda_{ij})^2}{4\lambda_{ij} k_B T}\right]$
  - J_{ij}: transfer integrals
  - $\Delta\mathcal{E}_{ij} = \Delta\mathcal{E}^{\text{el}} + \Delta\mathcal{E}^{\text{ext}}$: energy difference
  - $\Delta\mathcal{E}^{\text{el}} = \mathcal{E}_i - \mathcal{E}_j$: difference in electrostatic energy
  - $\Delta\mathcal{E}^{\text{ext}} = q < \mathbf{F}, S_i - S_j >$: energy difference due to electric field

- Modeling of $\{\mathcal{E}_n, n \geq 1\}$
  - $\mathcal{E}_n \sim \mathcal{N}(m_{\mathcal{E}}, \sigma_{\mathcal{E}}^2)$ positively correlated in space:
  - $M_n^{(a)}, M_n^{(b)}, M_n^{(c)} \sim \mathcal{N}(0, \sigma_{\mathcal{E}}^2)$ iid $\Rightarrow$ 4−tuple $(S_n, M_n^{(a)}, M_n^{(b)}, M_n^{(c)})$
  - $S_{n,(1)}, S_{n,(2)}, \ldots, S_{n,(\ell)}$: ℓ nearest neighbors of S_n with RV $M_n^{(b),(i)}, M_n^{(c),(i)},\ i = 1, \ldots, \ell$

Modeling of edge weights Q

- Movement of charges according to Markov process
- $Q = \{Q_{ij}, (S_i, S_j) \text{ oder } (S_j, S_i) \in E\}$ transition rates
- $Q_{ij} = \frac{2\pi}{\hbar} \frac{J_{ij}^2}{\sqrt{4\pi\lambda_{ij} k_B T}} \exp\left[-\frac{(\Delta\mathcal{E}_{ij} - \lambda_{ij})^2}{4\lambda_{ij} k_B T}\right]$
  - J_{ij}: transfer integrals
  - $\Delta\mathcal{E}_{ij} = \Delta\mathcal{E}^{el} + \Delta\mathcal{E}^{ext}$: energy difference
  - $\Delta\mathcal{E}^{el} = \mathcal{E}_i - \mathcal{E}_j$: difference in electrostatic energy
  - $\Delta\mathcal{E}^{ext} = q < \mathbf{F}, S_i - S_j >$: energy difference due to electric field

- Modeling of $\{\mathcal{E}_n, n \geq 1\}$
  - $\mathcal{E}_n \sim \mathcal{N}(m_\mathcal{E}, \sigma_\mathcal{E}^2)$ positively correlated in space:
  - $M_n^{(a)}, M_n^{(b)}, M_n^{(c)} \sim \mathcal{N}(0, \sigma_\mathcal{E}^2)$ iid $\Rightarrow$ 4−tuple $(S_n, M_n^{(a)}, M_n^{(b)}, M_n^{(c)})$
  - $S_{n,(1)}, S_{n,(2)}, \ldots, S_{n,(\ell)}$: ℓ nearest neighbors of S_n with RV $M_n^{(b),(i)}, M_n^{(c),(i)}, \; i = 1, \ldots, \ell$
  - $\mathcal{E}_n = \sqrt{\omega_a} M_n^{(a)} + \sqrt{\frac{\omega_b}{\ell_b}} \sum_{i=1}^{\ell_b} M_n^{(b),(i)} + \sqrt{\frac{1-\omega_a-\omega_b}{\ell_c}} \sum_{i=1}^{\ell_c} M_n^{(c),(i)} + m_\mathcal{E}$
    $\omega_a, \omega_b \geq 0$ $(\omega_a + \omega_b \leq 1)$, $\ell_b, \ell_c > 0$.

Modeling of Edge Weights Q

Modeling of Edge Weights Q

- Modeling of $\{J_{ij}^2\}$

Modeling of Edge Weights Q

- Modeling of $\{J_{ij}^2\}$
- $J_{ij}^2 = \exp(\mathrm{X_{ij}})$ with $X_{ij} \sim \mathcal{N}\left(m_{g_1}(d\left(S_i, S_j\right)), \sigma_{g_2}^2((S_i, S_j))\right)$.
- $m_{g_1}, \sigma_{g_2}^2$ polynomials of degrees g_1, g_2 with $\sigma_{g_2}^2(r) > 0$ for all $r_{\min} \leq r \leq r_{\max}$.

Application

Application

- Modeling of charge transport in amorphous molecular systems

Application

- Modeling of charge transport in amorphous molecular systems
- Understanding of elementary processes necessary to improve (organic) electronic systems

Application

- Modeling of charge transport in amorphous molecular systems
- Understanding of elementary processes necessary to improve (organic) electronic systems
- Mobility: $\xi = \frac{v}{|\mathbf{F}|}$
  - v velocity of electrons under steady-state
  - $|\mathbf{F}|$ strength of the electric field

Application

- Modeling of charge transport in amorphous molecular systems
- Understanding of elementary processes necessary to improve (organic) electronic systems
- Mobility: $\xi = \frac{v}{|\mathbf{F}|}$
  - v velocity of electrons under steady-state
  - $|\mathbf{F}|$ strength of the electric field
- Fitting to reference systems gained by atomistic molecular simulations (Max-Planck-Institute for Polymer Research)

Application

- Modeling of charge transport in amorphous molecular systems
- Understanding of elementary processes necessary to improve (organic) electronic systems
- Mobility: $\xi = \frac{v}{|\mathbf{F}|}$
  - v velocity of electrons under steady-state
  - $|\mathbf{F}|$ strength of the electric field
- Fitting to reference systems gained by atomistic molecular simulations (Max-Planck-Institute for Polymer Research)
  - morphology of 4096 molecules simulated

Application

- Modeling of charge transport in amorphous molecular systems
- Understanding of elementary processes necessary to improve (organic) electronic systems
- Mobility: $\xi = \frac{v}{|\mathbf{F}|}$
  - v velocity of electrons under steady-state
  - $|\mathbf{F}|$ strength of the electric field
- Fitting to reference systems gained by atomistic molecular simulations (Max-Planck-Institute for Polymer Research)
  - morphology of 4096 molecules simulated
  - large computational effort

Application

- Modeling of charge transport in amorphous molecular systems
- Understanding of elementary processes necessary to improve (organic) electronic systems
- Mobility: $\xi = \frac{v}{|\mathbf{F}|}$
  - v velocity of electrons under steady-state
  - $|\mathbf{F}|$ strength of the electric field
- Fitting to reference systems gained by atomistic molecular simulations (Max-Planck-Institute for Polymer Research)
  - morphology of 4096 molecules simulated
  - large computational effort
  - analysis of larger systems desired

Application

- Modeling of charge transport in amorphous molecular systems
- Understanding of elementary processes necessary to improve (organic) electronic systems
- Mobility: $\xi = \frac{v}{|\mathbf{F}|}$
  - v velocity of electrons under steady-state
  - $|\mathbf{F}|$ strength of the electric field
- Fitting to reference systems gained by atomistic molecular simulations (Max-Planck-Institute for Polymer Research)
  - morphology of 4096 molecules simulated
  - large computational effort
  - analysis of larger systems desired
  - stochastic model approx. factor 10.000 faster

Model fitting to DCV4T

Model fitting to DCV4T

- Output molecular simulation: Graph $G^{\text{Mol}} = (V^{\text{Mol}}, E^{\text{Mol}}, Q^{\text{Mol}})$

Model fitting to DCV4T

- Output molecular simulation: Graph $G^{\mathrm{Mol}} = (V^{\mathrm{Mol}}, E^{\mathrm{Mol}}, Q^{\mathrm{Mol}})$
- Fitting point process

Model fitting to DCV4T

- Output molecular simulation: Graph $G^{\text{Mol}} = (V^{\text{Mol}}, E^{\text{Mol}}, Q^{\text{Mol}})$
- Fitting point process
  - intensity $\widehat{\lambda} = \frac{|V^{\text{Mol}}|}{\nu_d(W)}$

Model fitting to DCV4T

- Output molecular simulation: Graph $G^{\mathrm{Mol}} = (V^{\mathrm{Mol}}, E^{\mathrm{Mol}}, Q^{\mathrm{Mol}})$
- Fitting point process
  - intensity $\widehat{\lambda} = \frac{|V^{\mathrm{Mol}}|}{\nu_d(W)}$
  - $L_n = r_{\mathrm{min}} + X_n$, $X_n \sim \Gamma(\iota_1, \iota_2)$

Model fitting to DCV4T

- Output molecular simulation: Graph $G^{\text{Mol}} = (V^{\text{Mol}}, E^{\text{Mol}}, Q^{\text{Mol}})$
- Fitting point process
  - intensity $\widehat{\lambda} = \frac{|V^{\text{Mol}}|}{\nu_d(W)}$
  - $L_n = r_{\min} + X_n$, $X_n \sim \Gamma(\iota_1, \iota_2)$
  - $D : [0, \infty) \to [0, 1]$ nearest-neighbor distance distribution function

Model fitting to DCV4T

- Output molecular simulation: Graph $G^{\mathrm{Mol}} = (V^{\mathrm{Mol}}, E^{\mathrm{Mol}}, Q^{\mathrm{Mol}})$
- Fitting point process
  - intensity $\widehat{\lambda} = \frac{|V^{\mathrm{Mol}}|}{\nu_d(W)}$
  - $L_n = r_{\min} + X_n$, $X_n \sim \Gamma(\iota_1, \iota_2)$
  - $D : [0, \infty) \to [0, 1]$ nearest-neighbor distance distribution function
  - $\int_{r_1}^{r_n} \left(D_{(\iota_1,\iota_2)}(r) - D^{\mathrm{Mol}}(r)\right)^2 \mathrm{d}r \to \min$

Model fitting to DCV4T

- Output molecular simulation: Graph $G^{\text{Mol}} = (V^{\text{Mol}}, E^{\text{Mol}}, Q^{\text{Mol}})$
- Fitting point process
  - intensity $\widehat{\lambda} = \frac{|V^{\text{Mol}}|}{\nu_d(W)}$
  - $L_n = r_{\min} + X_n$, $X_n \sim \Gamma(\iota_1, \iota_2)$
  - $D : [0, \infty) \to [0, 1]$ nearest-neighbor distance distribution function
  - $\int_{r_1}^{r_n} \left(D_{(\iota_1,\iota_2)}(r) - D^{\text{Mol}}(r)\right)^2 \mathrm{d}r \to \min$
- Fitting edge model
  - Estimate $p^{\text{Mol}}(r) = P\left(S_i, S_j \text{ connected } \| d(S_i, S_j)\right)$

Model fitting to DCV4T

- Output molecular simulation: Graph $G^{\text{Mol}} = (V^{\text{Mol}}, E^{\text{Mol}}, Q^{\text{Mol}})$
- Fitting point process
  - intensity $\widehat{\lambda} = \frac{|V^{\text{Mol}}|}{\nu_d(W)}$
  - $L_n = r_{\min} + X_n,\ X_n \sim \Gamma(\iota_1, \iota_2)$
  - $D : [0, \infty) \to [0, 1]$ nearest-neighbor distance distribution function
  - $\int_{r_1}^{r_n} \left(D_{(\iota_1,\iota_2)}(r) - D^{\text{Mol}}(r)\right)^2 \mathrm{d}r \to \min$
- Fitting edge model
  - Estimate $p^{\text{Mol}}(r) = P\left(S_i, S_j \text{ connected } \| d(S_i, S_j)\right)$
  - fitting of p_g an p^{Mol}.

Model fitting to DCV4T

- Output molecular simulation: Graph $G^{\text{Mol}} = (V^{\text{Mol}}, E^{\text{Mol}}, Q^{\text{Mol}})$
- Fitting point process
  - intensity $\widehat{\lambda} = \frac{|V^{\text{Mol}}|}{\nu_d(W)}$
  - $L_n = r_{\min} + X_n$, $X_n \sim \Gamma(\iota_1, \iota_2)$
  - $D : [0, \infty) \to [0, 1]$ nearest-neighbor distance distribution function
  - $\int_{r_1}^{r_n} \left(D_{(\iota_1,\iota_2)}(r) - D^{\text{Mol}}(r)\right)^2 \mathrm{d}r \to \min$
- Fitting edge model
  - Estimate $p^{\text{Mol}}(r) = P\left(S_i, S_j \text{ connected } \| d(S_i, S_j)\right)$
  - fitting of p_g an p^{Mol}.
- fitting of model for edge weights

Model fitting to DCV4T

- Output molecular simulation: Graph $G^{\mathrm{Mol}} = (V^{\mathrm{Mol}}, E^{\mathrm{Mol}}, Q^{\mathrm{Mol}})$
- Fitting point process
  - intensity $\widehat{\lambda} = \frac{|V^{\mathrm{Mol}}|}{\nu_d(W)}$
  - $L_n = r_{\min} + X_n,\ X_n \sim \Gamma(\iota_1, \iota_2)$
  - $D : [0,\infty) \to [0,1]$ nearest-neighbor distance distribution function
  - $\int_{r_1}^{r_n} \left(D_{(\iota_1,\iota_2)}(r) - D^{\mathrm{Mol}}(r)\right)^2 \mathrm{d}r \to \min$
- Fitting edge model
  - Estimate $p^{\mathrm{Mol}}(r) = P\left(S_i, S_j \text{ connected } \| d(S_i, S_j)\right)$
  - fitting of p_g an p^{Mol}.
- fitting of model for edge weights
  - $m_{\mathcal{E}}, \sigma^2_{\mathcal{E}}$ ML estimator
  - $\kappa : [0,\infty) \to [-1,1]$: mark correlation function
  - $\left(\widehat{\omega}_a, \widehat{\omega}_b, \widehat{\ell}_b, \widehat{\ell}_c\right) = \arg\min_{(\omega_a,\omega_b,\ell_b,\ell_c)} \int_{r_1}^{r_2} \left(\kappa(r) - \kappa_{(\omega_a,\omega_b,\ell_b,\ell_c)}(r)\right)^2 dr$

Validation

Validation point process

Validation

Validation point process

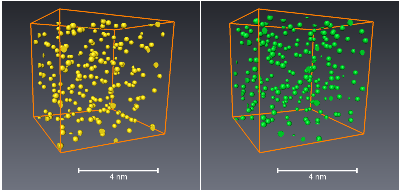

Validation

Validation point process

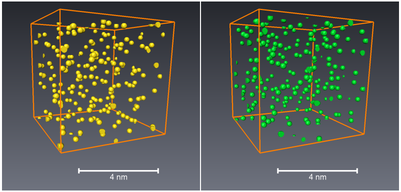

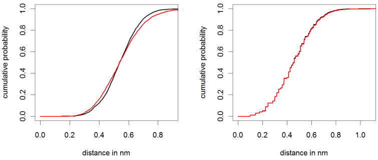

Validation

Validation point process

Validation graph

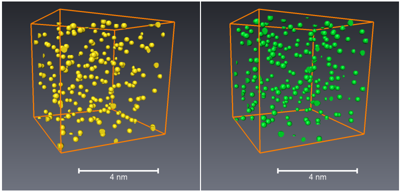

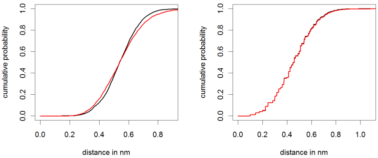

Validation

Validation point process

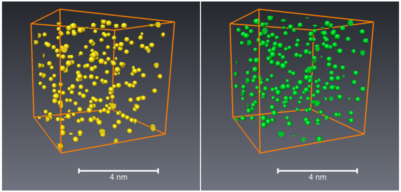

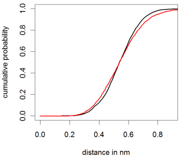

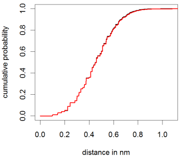

Validation graph

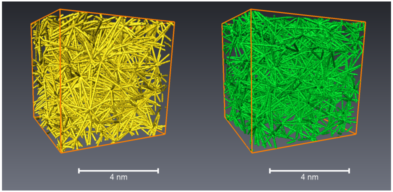

Validation

Validation point process

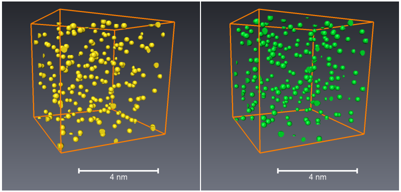

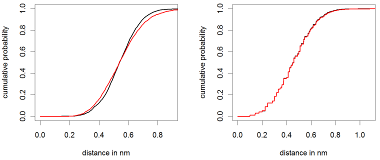

Validation graph

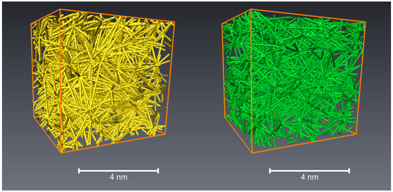

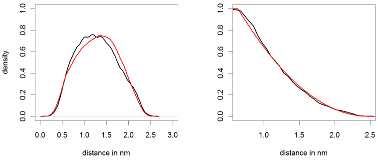

Validation

Validation charge transport

- Output stochastic model: Graph $G = (V, E, Q)$
- $M = \{M_t, t \geq 0\}$ Markov process (state space V, transition rates Q)
- $\widetilde{M} = \{\widetilde{M}_n, n \geq 0\}$: embedded Markov chain
- $N = \{N_t, t \geq 0\}$: counting process
- $v = \lim_{t \to \infty} \frac{1}{t} \sum_{n=0}^{N_t - 1} \mathbf{d}_{\widetilde{M}_n, \widetilde{M}_{n+1}}$: velocity

Validation

Validation charge transport

- Output stochastic model: Graph $G = (V, E, Q)$
- $M = \{M_t, t \geq 0\}$ Markov process (state space V, transition rates Q)
- $\widetilde{M} = \{\widetilde{M}_n, n \geq 0\}$: embedded Markov chain
- $N = \{N_t, t \geq 0\}$: counting process
- $v = \lim_{t \to \infty} \frac{1}{t} \sum_{n=0}^{N_t - 1} \mathbf{d}_{\widetilde{M}_n, \widetilde{M}_{n+1}}$: velocity

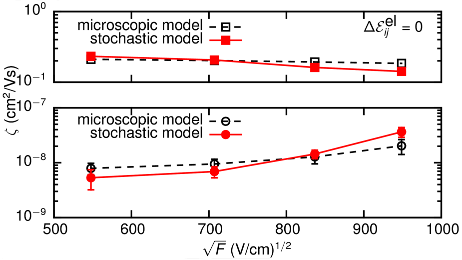

Stochastic Modeling on Microscopic Length Scale and Application of Graphite Electrodes

Simulated annealing for generation of microstructures

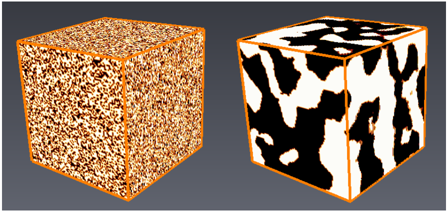

- Start with random allocation of voxels given volume fraction α
- Coarsening of morphology by interchanging voxels.
  - T temperature, $c(\cdot)$ cost function to be reduced (e.g. surface area)
  - Pick a pair of voxels at random
  - Swap voxels if cost function decreases, otherwise accept swap with probability $\exp\left(\frac{c(\text{no change})-c(\text{change})}{T}\right)$
  - Decrease T with time
- Stop if desired value of $c(\cdot)$ is reached.

Our approach: graph-based simulated annealing

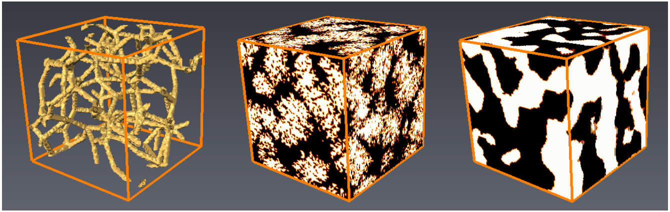

- Simulated annealing: simple but computational expensive, limited control of microstructure
- Hybrid approach: combining spatial stochastic graph modeling with simulated annealing
  - simulate random geometric graph
  - start configuration of voxels by project voxels onto the graph
  - run simulated annealing on new start configurations
  - voxels of graph fixed
- spatial graph serves as backbone of microstructure
- fast, good control on microstructure

Stochastic graph model

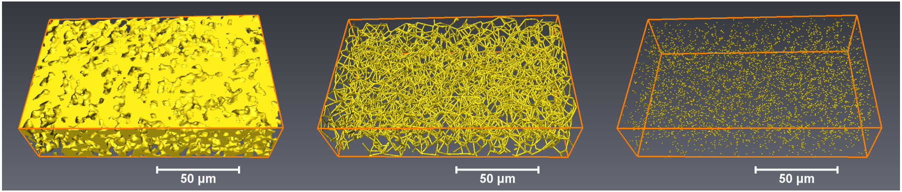

- Extract spatial graph (V, E) from experimental data by skeletonization
  - V set of vertices
  - E set of edges
- Stochastic modeling by
  - Point process model for the set of vertices
  - a stochastic model for setting edges
  - Fitting of model parameters to corresponding experimental data

Point process model: modulated hardcore point process

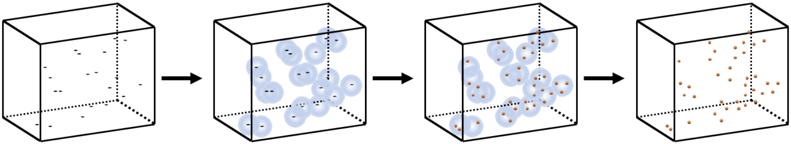

(1) Simulation of homogeneous Poisson process

(2) Simulation of Boolean Model

(3) Simulation of Poisson hardcore model inside the Boolean Model

Stochastic model for putting edges

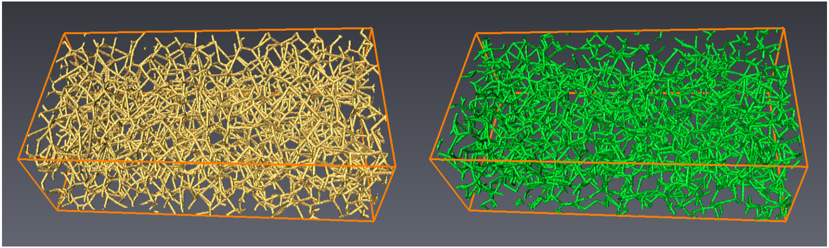

experimental graph (left) and simulated graph (right)

- Connecting nearest neighbors
  - Connect each point S_i with its n nearest neighbors.
  - Start with nearest neighbor
  - Connection is rejected if angle to previous edges undercuts a threshold γ_1
- Postprocessing of edges
  - If angles undercut threshold γ_2: deletion with probability $p \in (0, 1)$.
  - Control of angles

Summary of graph-based simulated annealing

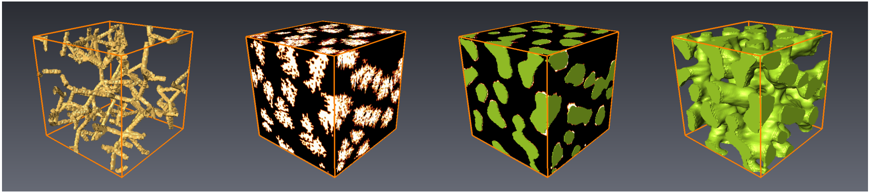

Synchroton tomography image data

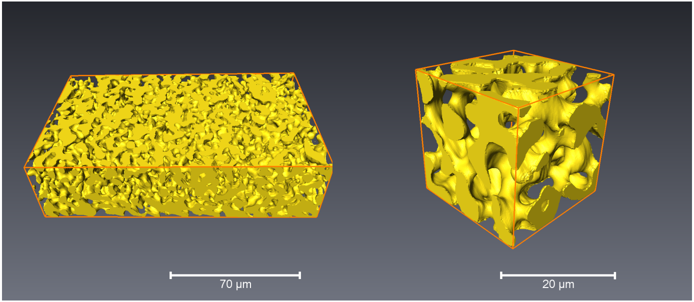

O. Stenzel *et al.*, Modelling and Simulation in Materials Science and Engineering, accepted

- 3D image of uncompressed graphite electrode used in Li-ion batteries
- tomography: Helmholtz Center Berlin, material: ZSW Baden-Württemberg
- yellow: graphite phase
- transparent: pore phase, volume fraction ca. 56%

Result: stochastic simulation model

- Modeling of the 3D morphology of graphite electrodes
- Size: $100 \times 100 \times 100$ voxels

Model validation

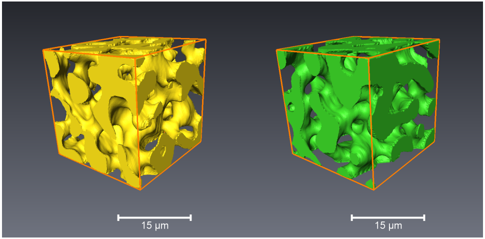

Cut-out of experimental (left) and simulated (right) microstructure

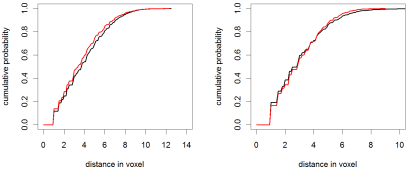

Spherical contact distribution from pore phase to graphite (left) and vice versa (right). Red curve displays experimental data and black curve simulated data.

Numerical results

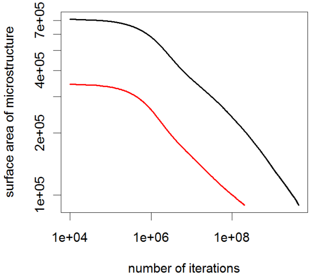

Surface area vs. the number of steps for standard simulated annealing (black) and graph-based simulated annealing (red)

- computational effort reduced to 5.81%

Two-stage voxel resolution

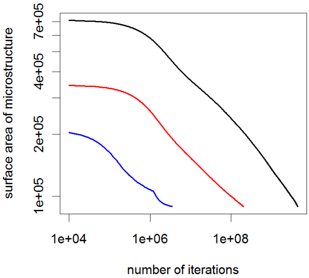

Surface area vs. the number of steps for standard simulated annealing (black), graph-based simulated annealing (red) and graph-based simulated annealing with two-stage voxel resolution (blue)

- computational effort reduced to 0.1%

O. Stenzel, D. Westhoff, I. Manke, M. Kasper, D. P. Kroese and V. Schmidt, Graph-Based Simulated Annealing: A Hybrid Approach to Stochastic Modeling of Complex Microstructures. Modelling and Simulation in Materials Science and Engineering **21** (2013), 055004